

IAC-18-D1,3,5,x45897

ROVER ORIENTATION ESTIMATION USING SUN SENSORS FOR LUNAR AND PLANETARY EXPLORATION

Takuto Oikawa

Tohoku University, Japan, oikawa@astro.mech.tohoku.ac.jp

Jasmin Bröhan

Hamburg University of Technology, Germany, jasmin.broehan@tuhh.de

Gabriel Dubernet

Ecole Nationale Supérieure des Sciences Appliquées et de Technologie de Lannion (ENSSAT), France,
dubernet.g.e@gmail.com

Kazuya Yoshida

Tohoku University, Japan, yoshida@astro.mech.tohoku.ac.jp

For space exploration rovers, knowing the exact local orientation is difficult due to the absence of Global Position System. From the global information (landing site) and the rovers images, the operator can make a rough estimation of its current position. Although this approach requires an active operator at all times, it is a very simple way of obtaining a position estimation. While the rover is in motion, wheel slippage is considered as it can be a source of heading error and diverge away from the intended motion plan. This problem is approached by tuning the wheel rotation speed based on the slip condition from terrestrial testing by mimicking the target environment. This method would be sufficient if the rover is landing at a pre-explored region such as the Apollo mission site. However, the above practice does not work when the rover travels to a previously unexplored area, or the condition of the explored lunar surface has changed over time. This results with the pre-tuned parameters will not be optimal for those cases. Therefore, we need a robust system that can track the rover's absolute orientation regardless of terrain conditions.

In this paper, we will present an approach using commercial off-the-shelf photodiodes as sun sensors. Arrays of diodes are added onto the rover; each installed on a different surface to measure all necessary directions. The calibration process is initially performed in a controlled environment with a single artificial sunlight emitter to measure the sensor's functionality. The test results are then compared with the outdoor condition to measure errors such as environmental noise from surface albedo. As a final validation process, a field test is conducted to show the rovers local orientation based on the sun heading. The rover's yaw estimation is during the turn maneuver operations, and the deviation is compared to the angle derived from the ground truth.

I. INTRODUCTION

Reliable feedback about motion estimation of a remotely operated vehicle that is 384,400 km away from the ground station operator with no Global Positioning System is critical for a successful exploration mission. For this, an accurate measurement of the roll, pitch, and yaw-angles is required at all times. In terrestrial application, a combination of the magnetometer and the six-axis inertial measurement units (IMU) are commonly used to measure the both the orientation and yaw estimation using quaternion with kalman filter technique^{1,2,3}. However, in lunar surface application such techniques do not work as the lunar magnetic field is very weak.

The lunar surface also has a challenging terrain, where the ground is filled with a loose particle layer, known as regolith. This type of terrain often has an issue where the wheels do not always contain grip, resulting in an unintended locomotive errors with slippage. Therefore, a sole usage of the six-axis IMU is not sufficient in yaw estimation as the gyroscope-data measurement accumulates the drift-errors over time. Usually this problem is approached by either developing vehicle dynamics defined by terramechanics theory and known soil parameter⁴ or utilizing sensors such as current measurements⁵ and wheel encoders^{6,7} to correct the slippage errors generated by the wheel-soil interaction.



Fig. 1: Flight model rover

Another approach to estimate the rover's motion and orientation under sandy terrain is to use a combination of the six-axis IMU and visual odometry^{8,9}. The orientation and position errors are typically low in this method. However, with the potential camera degradation from particle radiation, other sensors should also be studied to increase the rover's robustness in such application.

With the thin atmosphere surrounding lunar surface, the usage of sun sensors is effective to compute the rover's orientation. Similar sensors have been previously studied with satellite¹⁰ or even in rover operation^{11,12,13}. These sensors range from photodiode arrays to camera based application. Although one of them¹¹ has been actually used for Mars mission, further studies are required to validate the sensors to be useful for outer space sun condition.

This paper presents the integration of the sun sensors made from low cost commercial off-the-shelf (COTS) photodiodes for lunar surface rover application, shown in Figure 1. The first half of the paper consists of the calibration procedure of the sensors, tailored for near space condition sunlight condition. The second half of the paper explains the actual validation of the sensors both in indoor and outdoor conditions including field testing.

II. SENSOR DESIGNS

For the sensors to work in space application, several conditions need to be considered. This includes:

- ① Lighting intensity of approximately 130,000 lux
- ② Radiation tolerant
- ③ Temperature resistant in the expected mission environment
- ④ Survive launch environment

⑤ Operational in vacuum condition

To satisfy the above requirement, a simple system is preferred that does not require any special handling to survive the space qualification testing. Among them, we focused the case 1 to determine the sensor that does not saturate at the given lighting condition. In this point of view, COTS photodiode was chosen instead of a linear photodiode array with a slit design¹⁰.

To determine the minimum number of installed photodiodes on the rover, we chose the photodiode that is capable of detecting 180 degrees field of view. This allows a minimum number of five orthogonal direction sensors attached on different rover surfaces (front, left, right, back and top side). From the measured sensor outputs on each surface, the azimuth and elevation angle of the sun can be calculated. The sensors are mounted with a 3D printed interface to ensure a normal heading direction on the surface. As a COTS sensor the silicon PIN photodiode SFH 203 P from OSRAM OPTO SEMICONDUCTORS is used. The computation of the sun incident angle from different voltages is performed by an ARM based microcontroller, where each of the photodiodes are read from a 16-bit analog-to-digital (ADC) converter. To estimate the overall position of the sun, in each iteration the two diodes with the highest voltage output are considered. With these two values the overall angle is calculated by

$$\theta_{total} = (\alpha_1 + \theta_1) \cdot w_1 + (\alpha_2 - \theta_2) \cdot w_2 \quad [1]$$

, where α_1 and α_2 are the angle associated to the sensors' heading direction on the system's coordinate frame, θ_1 and θ_2 are the incident angle between the corresponding sensor's heading direction and the sun, and w_1 and w_2 are the weight factors for the respective sensor, where the sum of the two weighted factors are always equal to one. We define that α_1 is the angle associated with the sensor that detects the highest output measurement from the ADC between the two sensors. The weighted factors are determined based on the calibration results from both indoor and outdoor testing in Section 3.

III. SENSOR CALIBRATION PROCESS

III.i Experimental Setup

To validate the system functionality, tests were conducted in a controlled environment, in form of a single light source in a magnetically shielded closed room. For this purpose, a SOLAX XC-500E artificial sunlight emitter was placed in front of a quadratic

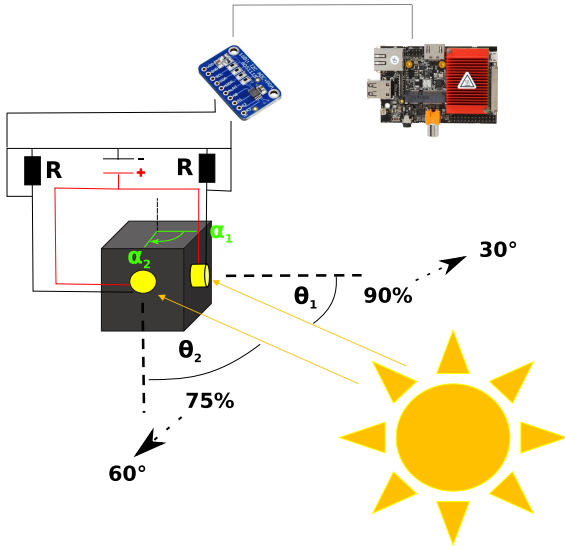


Fig. 2: Schematic diagram of the sensor system and the data acquisition method

wooden block, covered in a light absorbent black metallic sheet to reduce reflection, holding the photodiodes in a 90° -angles to each other (Figure 3). With a rotation table, the photodiodes are exposed to different light incident angles.

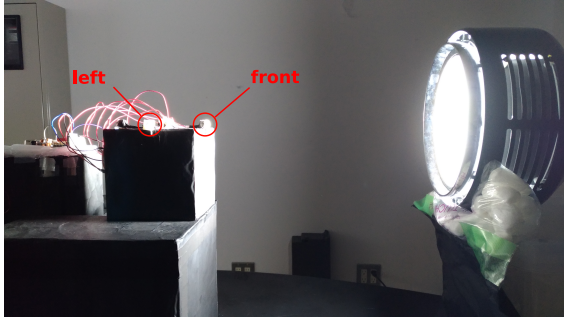


Fig. 3: Controlled Environment with a SOLAX XC-500E artificial sunlight emitter and diodes allocated in 90° -angle

III.ii Calibration Results

For indoor application, the calibration for the normalization of the voltage is done by facing the light source with one diode in a 0° -angle to gain a maximum voltage, which is then used during the whole test run. For outdoor application the value of the diode on the top in combination with the wanted sun elevation angle taken from sun position data for the specific day is used and updated every 30 seconds. We assume

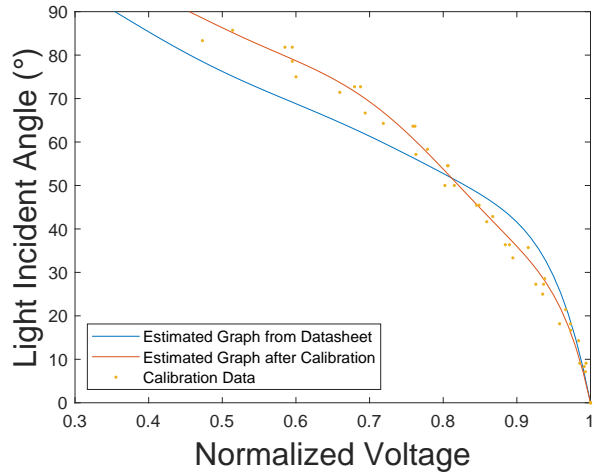


Fig. 4: Determined dependence of normalized voltage and light incident angle

that the rover's motion is on a two-dimensional flat ground.

As indicated in the datasheet, the photodiodes have a normal-distribution shaped dependence between the light incident angle and the normalized output voltage. To prove this, several test runs were conducted. As indicated in Figure 4, the data sets were compared to an estimated curve from the datasheet, and finally a new curve was created, using the MATLAB Curve Fitting Toolbox. The equation (see equation 2) is used to calculate the light incident angle $\theta_{incident}$ of each photodiode's normalized output voltage U_{out} .

$$\begin{aligned} \theta_{incident} = & p_1 \cdot U_{out}^9 + p_2 \cdot U_{out}^8 + p_3 \cdot U_{out}^7 + p_4 \cdot U_{out}^6 \\ & + p_5 \cdot U_{out}^5 + p_6 \cdot U_{out}^4 + p_7 \cdot U_{out}^3 + p_8 \cdot U_{out}^2 \\ & + p_9 \cdot U_{out} + p_{10} \end{aligned} \quad [2]$$

To show the validity of the yaw computation, we conducted a 360° -turn in the indoor and outdoor test environment. The purpose of the outdoor test is to determine the effect of the albedo to the sensor from the surface. For each test run, we align the front diode normal to the light source (the artificial emitter for indoor and the sun for outdoor). The results for both cases are shown in Figure 5. For the indoor testing, The sensors were able to compute the azimuth angle within 10 degrees of accuracy. For the outdoor case, we were able to achieve up to 15 degrees of accuracy. We can expect that the surface reflection has increased the errors for outdoor test-

Name	p_1	p_2	p_3	p_4	p_5	p_6	p_7	p_8	p_9	p_{10}
Datasheet	-8525	18355	-4563	-13184	3861	11564	-10929	4041	-791	171
Calibrated	-21571	48730	-8411	-46460	7403	59928	-60389	25320	-5043	493

Table 1: Polynomial fit curve values of the photodiode sensors.

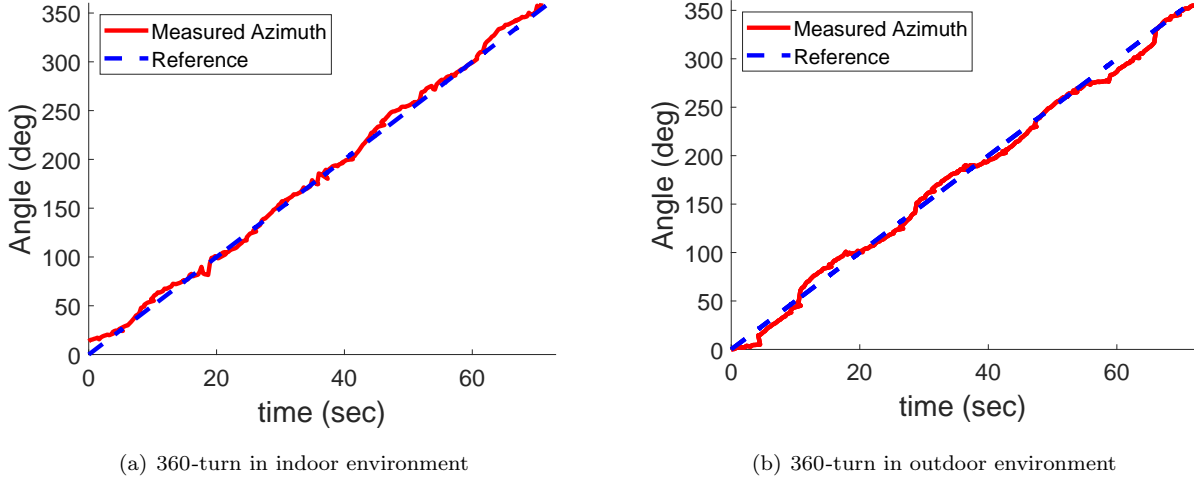


Fig. 5: Azimuth testing results using the rotating table

ing. To account the with and without albedo effect, we tuned the weight factors as $w_1 = 0.4$ and $w_2 = 0.6$ for indoor and $w_1 = 0.3$ and $w_2 = 0.7$ for outdoor testing.

IV. FIELD TESTING AND RESULTS

Field Test was conducted at the beach near Sendai city on August 23, 2018 at coordinate 38.2597°N, 141.0178°E. Figure 6 shows the rover's test setup. This rover has two LTE networks, omnidirectional camera, five different cameras (four of them for 360 degrees views and one for heaven-sighted view), micro-controllers, and real-time kinematic (RTK) GPS for ground truth. For the yaw estimation experiment, the photodiodes and the RTK GPS are only used.

To validate the yaw computation based on the five photodiodes, the rover travelled in a opened C shaped trajectory, shown in Figure 7. This path has three different curve points throughout the test, allowing to assess the rover's heading angle.

The rover's azimuth angle is computed as follows. We define that the rover's azimuth angle is rotating on a counterclockwise direction, shown in Figure 7. The field test was conducted on a relatively flat surface; thus, the rover is assumed to rotate on a

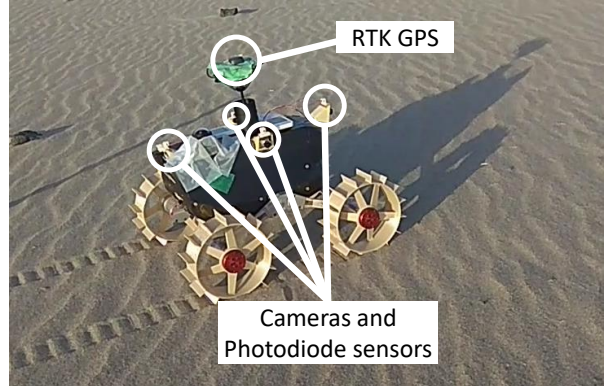


Fig. 6: Test setup on the rover

two-dimensional plane. Throughout the test, a small specks of cloud were observed. This created a shade on the ground on a certain time, resulting in a decrease in voltage measurement for all sensors. Due to the non-constant lighting condition, computing elevation angle based on the top surface photodiode sensor alone becomes very difficult. As an alternative approach, we determine the elevation angle based on the sun's position during the field testing time. From the LTE connection, the micro-controller tracks the

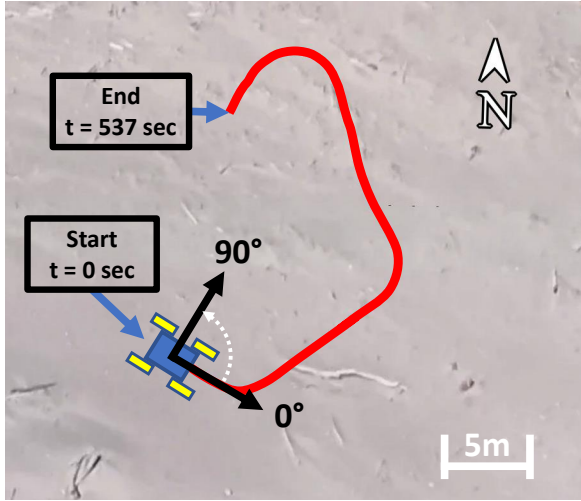


Fig. 7: Rover's Trajectory during the field test.
The path is mapped via Google Map
©GOOGLE

time while the rover is in operation. By comparing the sun's path and the time of the day, we can estimate the elevation angle. From the obtained elevation angle and the measured voltage output from the top surface photodiode, the expected maximum voltage output for other four photodiodes can be calculated using the voltage-angle relationship derived from Figure 4. This value is then used to normalize every output to compute the azimuth angle using the equation 1.

During the testing, we noticed that the rover's azimuth angle did not match precisely when we used the indoor testing weighting factor. We believe that this error comes from the shade generated by the cloud, where the sensors' output is skewed. From the obtained date in the test run, we processed the data by analyzing each measured sensor outputs. To improve the azimuth computation, we have tuned the weighted factor derived from equation 1, and chose w_1 as 0.3 and w_2 as 0.7 respectively, which is a similar result from the outside test during the calibration procedure.

The result with the rover's yaw rotation and the ground truth is shown in Figure 8. Throughout the test, the sun sensors were able to detect whenever the rover starts the turn maneuver. Overall, the rover's yaw estimation was computed at within 15 degrees during most of the test run. However, at certain region, the rover had a maximum error of 22 degrees. Other than the shade issue, the slight difference in the output from each photodiode may have deviated

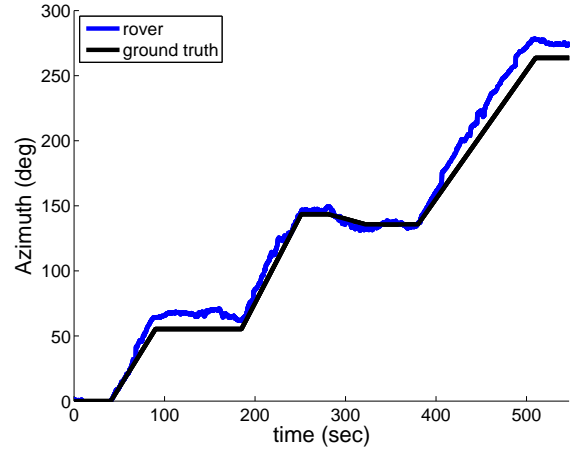


Fig. 8: Change in azimuth angle during the rover's run in field test.

the azimuth computation. By re-calibrating each of the sensor's behavior, sensor output can be improved for the specific cases.

V. CONCLUSION

Using a readily available COTS photodiode, the rover is capable of detecting its' yaw orientation in real-time operation. In the controlled lunar lighting condition, we have demonstrated that the photodiodes are capable of measuring the yaw at a error of less than 10 degrees. From the field testing, the rover's yaw estimation did not perform as well as expected in certain rover's orientation.

To improve the solar elevation angle measurement in real-time, we plan to use the heaven-headed camera to track the sun's position using computer vision technique. For future work, we plan to add the six-axis IMU data to calculate the rover's orientation for run in sloped terrain.

ACKNOWLEDGMENTS

This research is partially funded by the Tohoku University Division for Interdisciplinary Advanced Research and Education.

¹X. Yun et al., "A Simplified Quaternion-Based Algorithm for Orientation Estimation from Earth Gravity and Magnetic Field Measurements," IEEE Transactions on Instrumentation and Measurement, vol. 57, no. 3, March 2008, pp. 638-650.

²Z. Tang et al., "Measurement and Estimation of 3D Orientation using Magnetic and Inertial Sensors," Advanced Biomedical Engineering, vol. 4, 2015, pp. 135-143.

³A. Sabatini, "Quaternion-Based Extended Kalman Filter for Determining Orientation by Inertial and Magnetic Sensing," IEEE Transactions on Biomedical Engineering, vol. 53, no. 7, July 2006 pp. 1346-1356.

⁴G. Ishigami et al., "Terramechanics-Based Model for Steering Maneuver of Planetary Exploration Rovers on Loose Soil," Journal of Field Robotics, vol. 24, no. 3, 2007, pp. 233-250.

⁵L. Ojeda et al., "Current-Based Slippage Detection and Odometry Correction for Mobile Robots and Planetary Rovers" IEEE Transactions on Robotics, vol. 22, no. 2, April 2006, pp. 366-378.

⁶G. Reina et al., "Slip-compensated path following for planetary exploration rovers," IEEE/ASME Transactions on Mechatronics, vol. 11, no. 2, April 2006, pp. 185-195

⁷K. S. Ali et al., "Attitude and position estimation on the Mars exploration rovers," in Proceedings 2005 IEEE International Conference on Systems, Man and Cybernetics, Oct. 2005, pp. 20-27.

⁸D. Helmick et al., "Slip-compensated path following for planetary exploration rovers," Advanced Robotics, vol. 20, no. 11, 2006, pp. 1257-1280.

⁹J. Yi et al., "Kinematic Modeling and Analysis of Skid-Steered Mobile Robots With Applications to Low-Cost Inertial-Measurement-Unit-Based Motion Estimation," IEEE Transactions on Robotics, vol. 25, no. 5, October 2009, pp. 1087-1097.

¹⁰M. A. Post et al., "A low-cost photodiode sun sensor for CubeSat and planetary microrover," International Journal of Aerospace Engineering, vol. 2013, Article ID 549080, 9 pages, 2013.

¹¹R. Volpe, "Mars rover navigation results using sun sensor heading determination," IEEE Transactions on Robotics and Automation, vol. 17, no. 6, January 2001, pp. 939-947.

¹²A. Trebi-Ollennu et al., "Design and Analysis of a Sun Sensor for Planetary Rover Absolute Heading Detection," in Proceedings 2005 IEEE International Conference on Systems, Man and Cybernetics, Oct. 2005, pp. 20-27.

¹³P. Frugale, et al., "Sun sensor navigation for planetary rovers: Theory and field testing," IEEE Transactions on Aerospace and Electronic Systems, vol. 47, no. 3, pp. 1631-1647, July 2011.